Date: Monday, Monday, 21 March 2017
For submission after review to: Journal of Power Sources

Sampled-time control of a microbial fuel cell stack

Hitesh C. Boghani, Richard M. Dinsdale, Alan J. Guwy, Giuliano C. Premier*

Sustainable Environment Research Centre (SERC), Faculty of Computing, Engineering and Science, University of South Wales, Pontypridd, Mid-Glamorgan, CF37 1DL, UK.

*Corresponding Author:
Prof Giuliano C. Premier
Phone: +44 (0)1443 482333
Fax: +44 (0)1443 482169
Email: iano.premier@southwales.ac.uk

Abstract

Research into microbial fuel cells (MFCs) has reached the point where cubic metre-scale systems and stacks are being built and tested. Apart from performance enhancement through catalysis, materials and design, an important research area for industrial applicability is stack control, which can enhance MFCs stack power output. An MFC stack is controlled using a sampled-time digital control strategy, which has the advantage of intermittent operation with consequent power saving, and when used in a hybrid series stack connectivity, can avoid voltage reversals. A MFC stack comprising four tubular MFCs was operated hydraulically in series. Each MFC was connected to an independent controller and the stack was connected electrically in series, creating a hybrid-series connectivity. The voltage of each MFC in the stack was controlled such that the overall series stack voltage generated was algebraic sum (1.26 V) of the individual MFC voltages (0.32, 0.32, 0.32 and 0.3). The controllers were able to control the individual voltages to the point where 2.52 mA was drawn from the stack at a load of 499.9 Ω (delivering 3.18 mW). The controllers were able to reject the disturbances and perturbations caused by electrical loading, temperature and substrate concentration.

Keywords: Microbial fuel cells; bioelectrochemical system; sampled-time control; digital control; stack voltage control; voltage reversal.

1. Introduction

Research into bioelectrochemical systems (BES) has expanded rapidly over the past 20 years [1]. BES technology can perhaps optimistically be gaged as standing at a technology readiness level (TRL) greater than 4, based on the evidence [2], that increasing deployment of larger-scale systems are being reported and trials of such processes are ongoing across the globe [3-6]. As practicality demands, these systems (represented by microbial fuel cells, (MFCs) in this study) need to be stacked to increase the voltage and reducing power performance to useful levels in the system. While electrically stacking MFCs in series is an obvious choice, it comes with the risk that one or more cells in the stack may experience voltage reversal [7-10], so causing deterioration in the performance of the entire stack. DC-DC converters offer the possibility of converting circa 0.3 volts to higher workable voltage (for example, 5 V). However, they tend to exhibit significant efficiency losses [11-15]. DC-DC converters serve to increase the cell or stack voltage, but do not necessarily offer the solution to cell voltage reversal within MFC stacks. Capacitor banks have been charged independently in parallel to the MFCs and discharged at a higher rate in series, boosting the voltage level [16, 17], and similarly with batteries. However, this involves significant actuations through electromechanical or solid state switches, related to the number of MFCs and storage devices. These operations may incur excessive I^2R power losses/consumption in operating the switching devices. A low power energy harvesting system may be a better choice in terms of the energy efficiency [12, 18, 19]. However, a suitable electrical connectivity needs to circumvent the losses that would arise due to the chemical reactions [9] in the event of voltage reversal in MFC stacks during operation.

It has been suggested that MFCs (typically tubular), connected hydraulically in series and sharing the anolyte, should not be connected electrically in series due to the possibility of , substrate cross-conduction effects [20] and the occurrence of a potential drop [21]. When interconnecting through the anolyte, it is suggested that they should rather be connected electrically in parallel. The deleterious effect of such liquid phase connectivity, may however be mitigated by the path length and conductivity of the anolyte. The issue of voltage reversal had been resolved previously where it was shown that by adopting a hybrid series connectivity of MFCs, voltage reversal could be avoided [22]. In parallel to each MFCs, a maximum power point tracking (MPPT) was connected and the electrical power was consumed in a resistive load. However, it was not clearly shown if the stack voltage generated this way, could reasonably be usable. It has also been shown that the voltage of MFCs can be controlled satisfactorily using a simple continuous time proportional + integral (PI) voltage controller along with a gain scheduling technique [23], but simultaneous stack connectivity and voltage control have not previously been shown.

MFCs produce power of the order of milli-watts and so their control and monitoring should be considered to have available only fractions of this power for their implementation, leaving the rest of the power available for other functions. Previous work on voltage control was implemented digitally, but the sampling time was relatively high in relation to the process dynamics and hence the control was effectively analogue, i.e. continuous control [23]. The likely implementation of control in MFCs will be through low cost, mask programmed microcontrollers. Continuous control would require relatively high frequency sampling to approximate analogue signals upon which Laplace s-domain control system design is based. An excessive proportion of the power generated by the MFCs would hence be consumed by the microprocessor based

control hardware. In comparison, the established field of sampled-time, true digital control in the z-domain is necessary in circumstances where the signals are only available periodically at time intervals, which are sufficiently long in comparison to the controlled process dynamics. However, true digital control can be accurate and effective in saving microprocessor power when using substantially sparse sampling intervals. Microcontrollers with specialised power saving functionality are currently commonplace. Several make available low power consumption *sleep modes*, hence the microcontroller can spend the large majority of its time in *sleep mode*, waking only to fulfil its control function in a minimum number of machine cycles, before resuming its *sleep mode*. Typically, during *sleep mode*, microcontrollers consume power of the order of μW [24] and hence this is advantageous for their implementation in MFC stacks. Such microcontrollers have been used by other researchers in order to harness power from MFCs to energise remote sensor elements [12] and for powering light emitting diodes (LEDs) [25].

A simple digital controller suitable for application with microcontrollers has here been investigated along with the hybrid connectivity strategy, which could be used to control/optimise the MFC stack. This study also shows for the first time that it is possible to connect electrically in series, the serially/hydraulically interconnected MFCs, whilst avoiding voltage reversal. The primary aim of the study is to investigate the possibility of using a sampled-time digital control strategy for the benefit of power saving. The use of digital resistors as actuators is expedient, but in practice, the power would be better utilised with appropriate power harvesting.

2. Materials and Methods

2.1 MFC construction and operation

Five MFC tubes consisting of five MFC modules were constructed by forming cation exchange membrane (CMI7000S, Membrane International Inc., NJ, USA) into six tubes as previously described in [23], although the length of the tubes differed and was 1.05 m in the current case. Thirty Pt catalysed air cathodes and thirty helical anodes were prepared as previously presented in [23]. Collectively, five cathodes were mounted (with 1 cm separation between them) on each of the membrane tubes. Five helical anodes were placed coaxially inside the tube assembly, aligning each with their corresponding cathode. This assembly is referred to as tube-*i* (i = 1, 2, … 5) in this text. Each of the MFC tube had an empty bed volume of 1.6 L approximately. Five of these tubes (containing 25 MFCs altogether) were connected to form two hydraulically/serially connected stacks of; 3 tubes (tube-1 to tube-3), and; 2 tubes (tube-4 and tube-5). Both stacks were fed in parallel from a common reservoir containing 16 L of standard media [26] with 40 mM sodium acetate (Figure 1c and Figure S1 in Supplementary Information, *(SI)*).

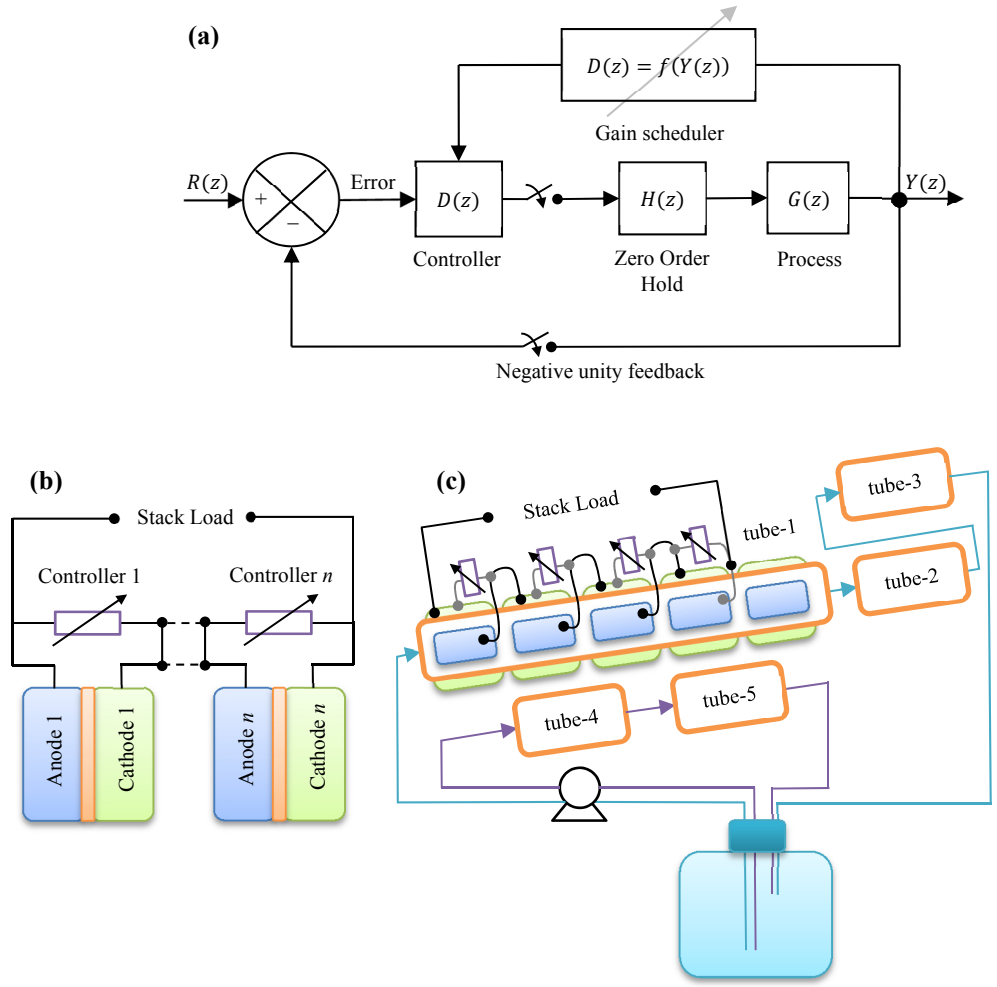

Figure 1. (a) Digital voltage controller scheme. (b) Simplified schematic of the MFC stack. (c) Schematic of the MFC stack (tube-2 – tube-5 are identical to tube-1).

A 20 L gas bag, filled with about 10 L of nitrogen, was attached on top of the reservoir in order to provide room to expand or contract in case of biochemical gas production or the withdrawal of liquid samples from the reservoir; so maintaining atmospheric pressure inside the reservoir. One of the tubes (tube-6) was not connected to the stack as it was being used elsewhere. The media was re-circulated from and to the reservoir, with a flow rate of 4.86 ± 0.04 mL min^{-1} and the stack was operated at room temperature of 22 ± 3 °C during the periods of acclimatisation/enrichment of the anodes. However, a higher flow rate of 9.5 mL min^{-1} was applied during the model identification of the MFCs and testing of the control strategy, i.e., the study presented

herein. MFCs were inoculated as previously described in [26]. Throughout the reported experimentation, the MFCs were operated in batch mode with re-circulation applied.

During the start-up phase of the MFCs, each were connected to 10 Ω electrically independent external loads, and were operated for about 9 months before their use in this study. The external loading was however, manually varied to the values of 1 kΩ, 100 Ω and 47 Ω during that 9 month period while impedance matching for peak power. During this study, all MFCs apart from those that were being controlled (first four MFC modules from the inlet end of tube-1), were normally connected to 47 Ω external loads, unless otherwise specified (for example, in the step tests).

2.2 MFC model identification

All MFCs in tube-1 were subjected to cumulative step changes in the electrical loading (Table 1) as an input disturbance as described previously in [23].

Table 1†. Parameters of the controller gain scheduling curve as shown in equation 5 and step input loading values that were used during the model identification.

	m	c	Step input loading (all in Ω)
$\boldsymbol{K_{p1}}$ for MFC1	0.0015	-0.1739	3.6, 7.2, 12, 19.2, 32.2, 73.8, 115.5
$\boldsymbol{K_{p2}}$ for MFC2	0.002	-0.1665	4.3, 7.9, 12.9, 19.9, 32.9, 75.4, 118.7
$\boldsymbol{K_{p3}}$ for MFC3	0.0022	-0.2248	5.5, 9.2, 13.9, 21.1, 34.3, 77.2, 120.4
$\boldsymbol{K_{p4}}$ for MFC4	0.003	-0.3037	6.5, 14, 22.4, 33.4, 51, 101.7, 149
MFC5			3.4, 7.4, 12.9, 21, 35.9, 83.9, 131.5

†Table shows two sets of data.

These disturbances occurred over the operating range of cell voltages (~0.2 to ~0.4 V). The electrical load (digital potentiometer, X9C102pz (Intersil® X9C102, Farnell UK Ltd., Leeds)) was controlled via a digital input/output module (NI 9403, National Instruments™, Newbury, UK), connected to a Microsoft® Windows® based compact data acquisition controller (NI cDAQ-9138, National Instruments™). The hardware was interfaced to the LabVIEW™ (National Instruments™) software algorithm for the execution of the control commands.

The data containing input loads and output voltages were recorded and used to identify 1st order models as shown in Equation 1.

$$V_{out}(t) = R_{in}k_{ss}\left(1 - e^{-t/\tau}\right)$$

Eq. 1

Where, V_{out} is voltage output at time *t,* R_{in} is the load input, k_{ss} is the steady-state gain and τ is the time constant in seconds. The model parameters were extracted by fitting the curve using Eq. 1 in MATLAB® (The MathWorks, Inc., Cambridge, UK), invoking command *LSQNONLIN*.

Four sets of dynamic models for each MFC were identified from temporally separated data occurring on day 2, 5, 7 and 9, when the anode substrate concentration was allowed to deplete over a 10 day period of batch mode operation (with recirculated flow applied as stated above).

2.3 Controller selection, parameterisation, and implementation

A simple Proportional + Integral (PI) controller was selected and the controller parameters were determined as elaborated previously in [23] but with Damping ratio (ζ) = 1. The control scheme was implemented in discrete-time (z-domain) as shown in Figure 1a where;

$$D(z) = K_p + \frac{K_i T z}{(z-1)} + K_d \frac{(z-1)}{Tz}$$

Eq. 2

$$\mathcal{Z}\{H(z)\} = \frac{1-e^{-sT}}{s}$$

Eq. 3

$$G(z) = \frac{1}{\tau} \cdot k_{ss} \cdot \frac{z}{z-e^{-T/\tau}}$$

Eq. 4.

$R(z)$ is the reference signal and $Y(z)$ is the output.

In eq. 2 – 4,

$D(z)$ is a three-term (proportional-integral-derivative) controller represented in z-domain where; K_p is proportional gain, K_i is integral gain, T is sampling period, K_d is derivative gain and z is e^{sT} in Laplace (s) domain, $H(z)$ is zero order hold, $G(z)$ is the process with steady-state gain k_{ss} and time constant τ.

In Equation. 2, K_d was removed from this study and set to 0; and K_i=1. The integral action was inherent in the actuator (digital potentiometer) implementation, as its resistance was cumulative with increment or decrement steps and did not require a continuous reference signal to hold the resistor value. So, in essence, the control strategy was implemented with proportional control only, assuming the integral action was derived from the digital potentiometric actuator. The actuator system was the same as previously described in [23].

The first four MFC modules in tube-1 were equipped with independent voltage controllers. The control parameters were scheduled as shown below.

$$K_p = mE + c$$

Eq. 5

Where; m and c are slope and intercept of the linear curve (as listed in Table 1) obtained by least square regression applied to the K_p values calculated for the piecewise linearised models of the MFCs; and E is instantaneous MFC voltage = Y.

The sampling period, T was scheduled in the controller using the following equation.

$$T = 0.3504\, e^{0.0119E}$$

Eq. 6

Eq. 6 was obtained by nonlinear regression applied to the sampling periods calculated for the piecewise linearized models of MFC1.

$$T_i = 0.35 \times \left[\frac{1}{10 f_{B_i}}\right]$$

Eq. 7

Where; T_i is the sampling period calculated for model i (=1, 2, 3, …, n), f_{B_i} is the bandwidth frequency = $0.35/t_{rise-time}$ with the rise-time, $t_{rise-time} = 2.2 \times \tau$; at a particular operating level. It may be noticed that the sampling time was 0.35 times faster than the ideal sampling period in order to avoid any undesirable outcome from the controller in case of sudden changes in the process. Herein, models from MFC1 were used for Eq. 6 as it exhibited the fastest dynamics in comparison to the models from MFC 2 – 4. As the controller was time multiplexed (sequentially applied to each MFC and executed through a single controller hardware), it was not possible to have different sampling periods scheduled for different MFCs in this study. However, this would not necessarily be the case if a separate microcontroller were used for each individual MFC module.

The first four MFCs (from the tube inlet end, MFC1-4) from MFC tube 1, were electrically connected in series as shown in Figure 1b. These may be visualised in Figure 1c. The electrode connection wires were physically passed through a cable gland at one end of the tube, and were then inter-connected through a junction box.

TEST 1 – Step tests: All MFCs were subjected to step inputs from 300 mV to 250 mV and from 250 mV to 350 mV. These were executed on all four MFCs at slightly different times with respect to each other but delayed by no more than 1 minute.

TEST 2 – Loading of the stack: Whilst MFC1, MFC3 and MFC4 were being controlled at 320 mV and MFC2 at 300 mV; the stack was sequentially loaded with the following electrical loads: 499.9 Ω, 10200 Ω, 9999 Ω, 1001 Ω, 801 Ω, 700 Ω, 600 Ω, 499.9 Ω, 400.6 Ω, 301 Ω and 499.9 Ω. The stack load was changed when reasonably steady states in the control loads (across each MFCs) were achieved. Here, the capacity of the control

to maintain the voltages of the MFC modules MFC1-4 within reasonable bounds was investigated.

TEST 3 – Extended test to investigate disturbance rejection: As in TEST 2 but with a constant stack loading of 499.9 Ω. This test continued for the 5 days immediately after TEST2.

24 hours before the beginning of TEST 2, the reservoir was replenished with standard media containing 40 mM of sodium acetate as the organic feed for the anodes and the system continued in batch mode (once more with re-circulation applied) until the end of TEST 3.

2.4 Analyses

The anodic liquid phase was sampled at the outlet end of tube-1 (end of MFC5) and the reservoir during MFC model identification and TEST 3. In order to sample the effluent from tube-1, Marprene® tubing (902.0064.016, Watson-Marlow Pumps Group, UK) at the end of the U-bend connecting outlet of tube-1 to the inlet of tube-2 was disconnected from the barbed connector and a sample (*circa* 30 mL) was allowed to flow into a 50 mL vessel. In addition, sampling from the reservoir was performed via a 100 mL syringe, withdrawing the liquid (*circa* 30 mL) through a Marprene® tube that was connected to the reservoir vessel through a bulkhead connector (WZ-06259-10, Cole-Parmer, UK), such that the reservoir vessel would not need to be opened. Before sampling from the reservoir, liquid was drawn into the syringe and pushed back into the reservoir with some force, at least three times, in order to facilitate a homogeneous sample.

The acetate concentration in the liquid was measured by the method described in [27],using a gas chromatograph (Clarus 500 GC, PerkinElmer, Inc., USA) in conjunction with an automated sampler (TurboMatrix HS 40, PerkinElmer, Inc.). The

sample was diluted four times in order to be within the measurement range of the Gas Chromatograph machine and the resultant value was re-adjusted by multiplying by 4.

The temperature and pH of the sampled liquid were measured using a pH electrode (LE438, Metler-Toledo International Inc., UK) connected to the pH meter (FG2 FiveGo™, Metler-Toledo International Inc.). Ionic conductivity of the sampled liquid was measured by using a conductivity electrode (LE703, Metler-Toledo International Inc.) connected to the conductivity meter (FG3 FiveGo™, Metler-Toledo International Inc.).

3. Results

3.1 MFC models

Figure 2a-e shows time constants and steady-state gains assuming first order process models adequately represent the MFCs at different operating points, analysed on day 2, 5, 7 and 9.

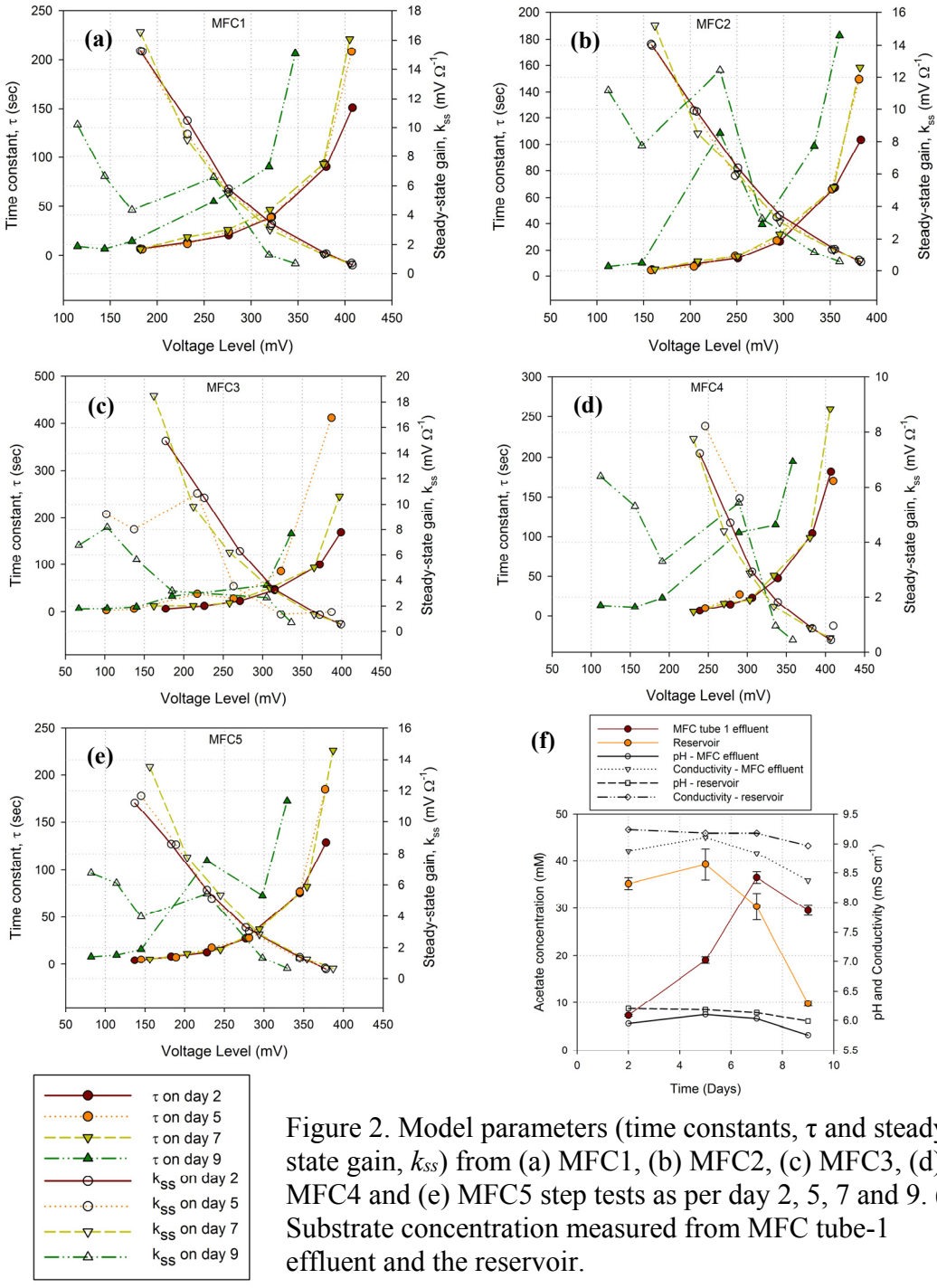

Figure 2. Model parameters (time constants, τ and steady-state gain, k_{ss}) from (a) MFC1, (b) MFC2, (c) MFC3, (d) MFC4 and (e) MFC5 step tests as per day 2, 5, 7 and 9. (f) Substrate concentration measured from MFC tube-1 effluent and the reservoir.

It appears that the time constants increased exponentially with an increase in the cell voltage, meaning that the MFC exhibited slower dynamics at higher voltages. Steady-state gains decreased in a decelerating fashion with increase in the operating level. However, controller performance results indicate that they can be reasonably represented by a straight line.

Figure 2f shows acetate concentration in the liquid sampled from the outlet end of the tube-1 and the reservoir. It is apparent that the acetate concentration in the effluent from tube-1 and the reservoir do no correlate. In fact, the MFC stack was operated in batch mode where the substrate in the reservoir was replaced once in a 2 weeks period. The inlet and outlet tubes terminated within the reservoir at same liquid level. When replenishing the substrate in the reservoir, liquid present within the MFCs were not replaced and so, the residual anode liquid volume from the MFCs would mix with the newly supplied feedstock. In addition, there may be anaerobic consumption of acetate by bacteria that may have grown in the reservoir bottle over the extended operation period. All or some of the factors mentioned above could account for the lack of correlation. However, it is clear that the MFC stack was given fresh medium through the reservoir with starting concentration of 40 mM and the substrate was allowed to deplete over the 10 days period during which the data for the models were obtained. The acetate concentration profile from the reservoir seems to align with the said methodology. The pH and conductivity of the liquid media varied between 5.76 – 6.2 and 8.37 – 9.24 mS cm^{-1} overall, respectively (Figure 2f).

3.2 Step tests and loading of the stack

Figure 3a shows the set points (SP) and resulting voltages from MFCs under the action of the controller. It can be observed that the MFC voltage responses exhibited overshoot of less than 9.9% overall as might be expected from marginally underdamped second order system. Figure 3b shows errors that were generated during the step tests, calculated efforts (in terms of number of potentiometer increment/decrement steps) and, applied loads in turn.

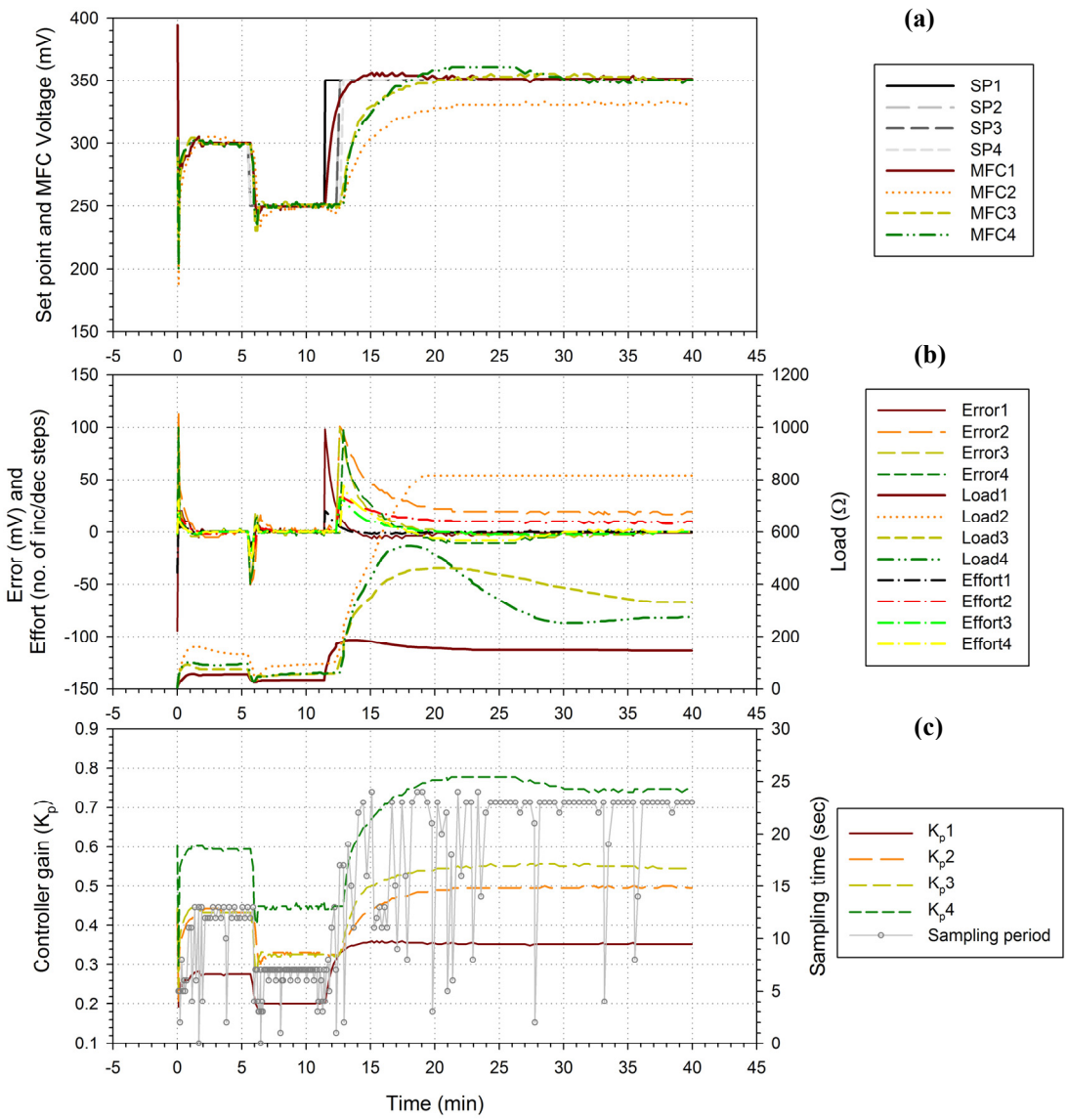

Figure 3. Plots showing (a) Set points (SP) and MFC voltages (b) Errors, Efforts and electrical loadings and, (c) controller gains and the controller sampling time during step tests.

No steady-state error was observed from any of the MFCs at any steps except for the MFC2 at SP of 350 mV. This was due to the saturation of its potentiometer, which had reached to its maximum range. Figure 3c shows proportional gain values that were calculated using the algorithm based on the Equation 5 that was supplied to the controller. Additionally, the sampling period is also shown. It can be seen that the sampling period and proportional gain values were selected/calculated by the algorithm to suit the operation conditions. When a MFC is operated at lower voltage levels, the

dynamics are faster relatively and the steady-state gains are higher in comparison to when operated at higher voltage levels. In summary, the sampling time needs to be faster and the controller gain needs to be lower when a MFC is operated at lower voltage levels, in comparison to when it is operated at higher voltage levels.

Controlling at very low voltage would mean that almost all of the power is consumed through the controller actuation, leaving none or limited levels of power to supply the stack load. Similarly, if MFCs were operated at very high or open circuit voltages, the controlling loads would always be at their maximum limit of range and therefore, would not be able to modulate the system, with consequent impaired capability for disturbance rejection by the controller. Hence, an intermediate set point (SP) of 320 mV was chosen on MFC1, 3 and 4; and the SP of 300 mV was chosen for MFC2 for the reasons mentioned above.

Figure 4a shows the SP and MFC voltages along with stack voltage. It can be observed that the stack voltage was indeed the algebraic sum of the cells connected in the stack, i.e. 1.26 V. Therefore, no voltage was lost whilst cells were in series. Figure 4b shows errors generated by the control algorithms. Figure 4c shows loads that were applied to each MFCs by their controllers, and stack load that was applied manually to the overall stack of four MFCs. It can be seen that the controllers were able to reject disturbances generated from the loading of the stack by adjusting their own loads. When the stack load was decreased from 400.6 Ω to 301 Ω, the controlling loads increased greatly, approaching their maximum range and therefore, the stack load was changed back to 499.9 Ω. This loading then continued for TEST 3.

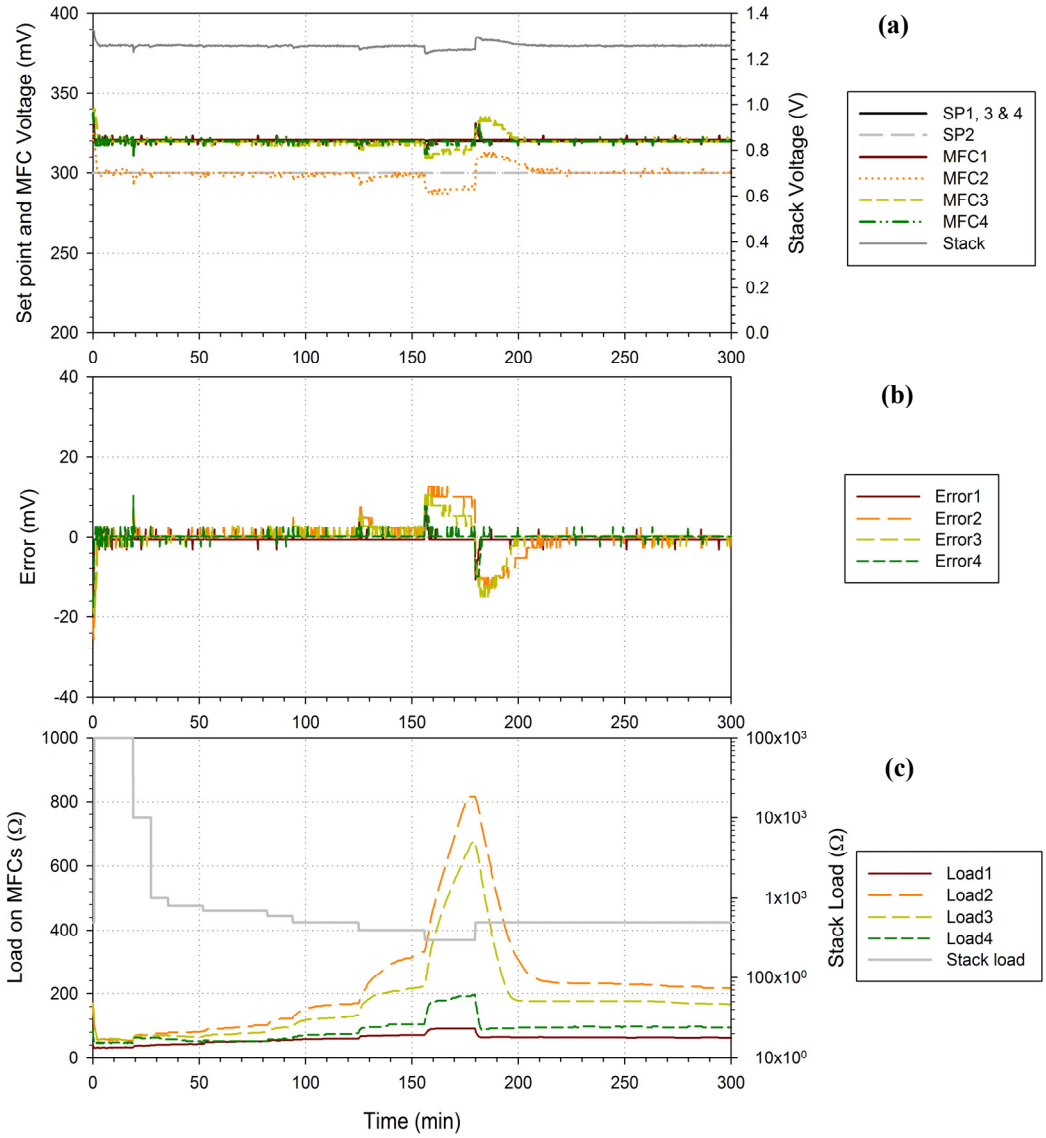

Figure 4. Plots showing (a) Set points (SP) and MFC voltages and stack voltage; (b) Errors and; (c) controller loadings and the stack loading during the stack-loading test.

3.3 Disturbance rejection

Figure 5a shows SP, MFC voltages and stack voltage when operated for a 5-day period whilst operating MFCs under batch mode as described. Figure 5b shows errors, which seem to oscillate up to ± 4 mV around 0. Also shown is the temperature of the liquid phase, periodically sampled, which remains between 20 and 22 °C.

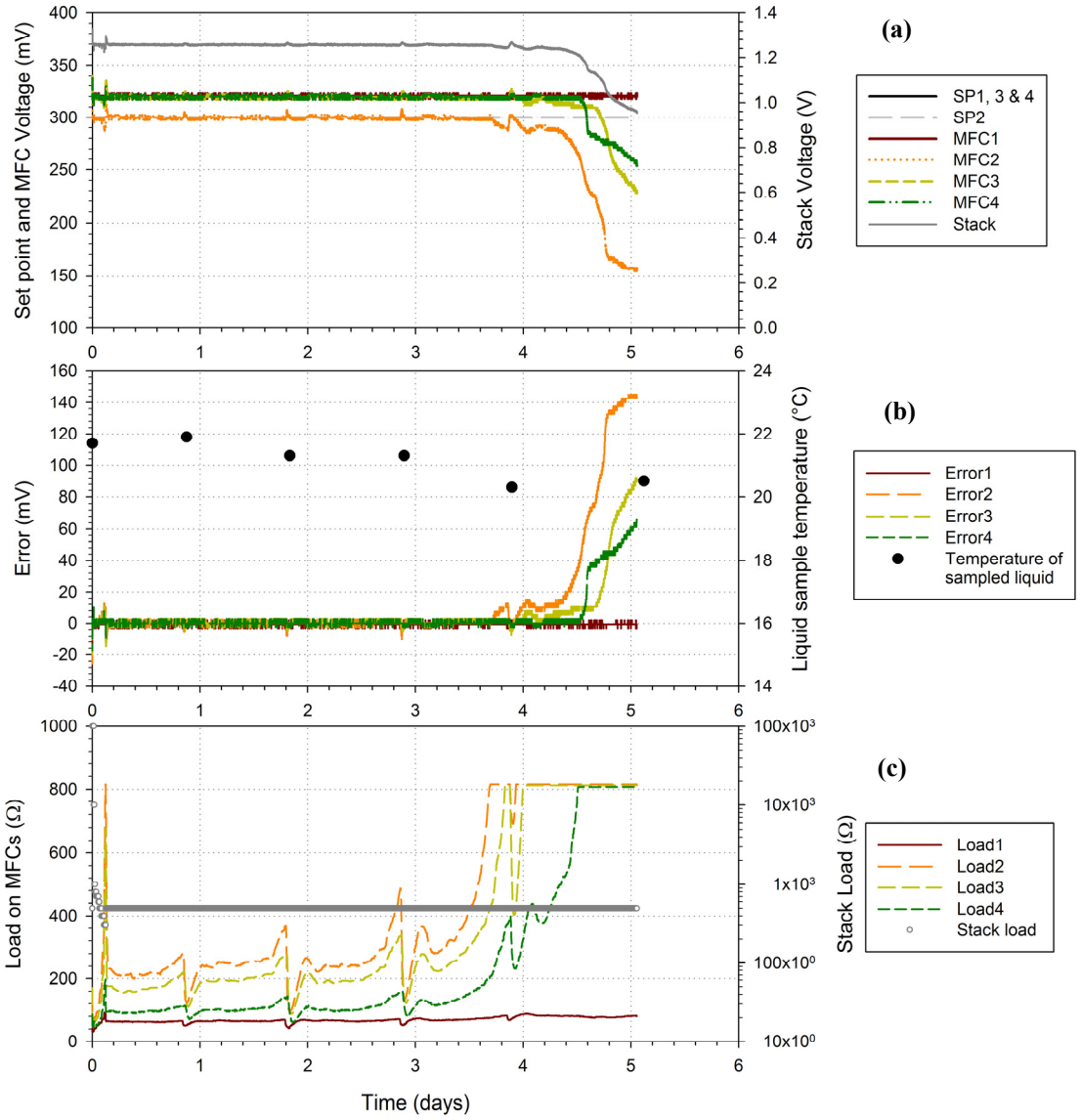

Figure 5. Plots showing (a) Set points (SP) and MFC voltages and stack voltage; (b) Errors and; (c) controller loadings and the stack loading during the long-term stack-loading test.

Online measurement of liquid phase and ambient temperature was not performed in this study, but previous measurements in similar circumstances suggest the diurnal variation in temperature produced discernible effect on the voltage (and/or current) output from the MFCs (Figure S3 in *SI*). While the ambient and liquid phase variations are small, it is worth noting that the expected fluctuations in MFC voltages from diurnal temperature variations were not evident, although the control action visible in the load variations are clearly periodic and diurnal (Figure 5c). Figure 5c also

shows a progressively increasing action represented by electrical loading loadings as the substrate depletes. While the perturbation on organic loading is not abrupt, it is persistent and continues to the point that control action saturates and no further restorative action is possible as insufficient substrate is present to generate the necessary current. Stack load was kept constant throughout TEST 3 and so, it can be seen that the MFC stack was able to deliver steady 1.26 V to a load of 499.9 Ω, generating steady power of 3.18 mW for a 4-day period.

4. Discussion

As bioelectrochemical systems are biologically catalysed, changes in their dynamic performance with time are likely because the microbial community can experience population shifts, growth, death, inhibition and metabolic variations in response to their environmental conditions. Once the biocatalyst has been selectively developed and becomes relatively established through acclimation, its catalytic performance may be maintained by ensuring the bacterial environment is relatively stable. Controlling the metabolic activities of the anode respiring bacteria by the regulation of the current sourced (electrons accepted) by the anode, is one method of sustaining the electroactive population. In practical systems, control of environmental conditions may be difficult or costly, but this work shows that a consistent BES performance can be engineered by modulating the electrical loading. This in turn can allow stacks of MFCs to operate without catastrophic voltage reversals or damage to the biocatalyst from electrical overloading and justifies the control functionality adopted. Furthermore, control functions can and should be achieved at low to moderate energy costs. Operating conditions can change considerably, even over the course of a day. Continuous time, gain scheduling adaptive control, has been shown previously to be a suitable strategy to deal with such environmental variability [23]. However, control

implementation must consume minimal power, and this can be achieved by reducing the computational effort. using Discrete time control with frequently sampling of the control variable (cell voltage), then determining the control action required and actuating the causal action, can all occur in the space of a few microseconds, and the control hardware can remain dormant (sleep mode) otherwise. The control performance evident in the results shows that the approach is practicable.

4.1 Sensitivity of MFC models to substrate concentration

This study has investigated how the variation of substrate concentration, (as may be evident in industrial effluents for example), affects the system dynamics. As shown in Figure 2a-e, all of the MFCs in tube-1 show no significant change in their time constants or steady-state gains during the first 7-day period, apart from the data points at highest voltage levels (~ 400 mV), at which the MFCs tend to saturate. 7 days after the replenishment of the substrate that the dynamics seem to change, possibly due to lack of an adequate amount of substrate (but this is related to the reservoir capacity). It is nevertheless interesting to note that most data seem to yield the same time constant as at the higher organic concentrations, except that a shift occurs to the level of achievable voltage at that lower organic concentrations. Substrate concentration and hence organic loading was the same for all four data sets and it has frequently been reported that as substrate depletes, the voltage drop across a static resistive load also decreases due to decreased current generation. Where the time constants deviated significantly from the main trend curve, it can be appreciated that the MFC response was not a time invariant 1^{st} order response. Rather, during the development of the 1^{st} order type responses, a change/switch occurred to follow an alternative 1^{st} order type trajectory (Figure S2 in *SI*). Notwithstanding this rapid change, in the controller design engineering, it was adequate to assume that as long as the system receive sufficient substrate, the dynamics

were unlikely to change significantly in a relatively short time periods of less than a month. Longer periods of several months or more have not been considered in this study, in terms of time variance of the dynamics.

4.2 Control of stack

The performance of the sampled-time control was assessed by performing closed-loop step tests (whilst the MFCs were under control). When there was no stack load connected (open circuit), all MFCs were controlled to their SPs apart from MFC2 as its load had reached its maximum and saturated. The MFC voltages were controlled within acceptable limits and cell voltage reversals were avoided by the architecture of the electrical connectivity, and the system's ability to cope with the disturbances (loading, temperature and substrate concentration) as shown by the results in Figure 3-5, is considered suitably accurate and responsive, within the limits of the applied perturbations. The control system's ability to respond to other perturbations could be studied further. However, better understanding of performance may result from on-site deployment in realistic conditions. Additionally, the process is nonlinear and to some unknown degree, time varying. Hence, the robustness and stability of the controller will be difficult to confirm with a high degree of certainty without operational experience. However, it seems that the controller was able to perform well in rejecting the disturbances generated by the loading (Figure 3 and Figure 4), substrate concentration and temperature (Figure 5). It is worth noting that the initial substrate concentration used was relatively high (~ 35 – 40 mM sodium acetate), depleting in the process of operation over 5 days. Because of the saturation limit of the external electrical load, lower starting concentration were not investigated, however it is expected that increasing the range of the external resistive load will sustain the MFC voltage to lower substrate concentration, with in the extreme, open circuit conditions. During TEST 2,

as higher current was demanded by the stack load (by lowering of the stack load resistance), and subsequent increases in the control effort on resistive loads can be observed, so limiting the current through the controller loads. It is likely that in the case of very high current demand, the controller loads could approach open circuit (very high resistive load) as in the case of MFC2 and MFC3. This is desirable as when the stack loading is demanded; the current needs preferably to be directed to meet that demand. The SPs were limited to around 300 mV as the controller loads would otherwise reach their maximum, which of course is easily remedied, but was not deemed necessary in this study. The proposed control strategy may be implementable with suitable energy harvesting circuitry such as the Texas Instruments, bq25504 (ultra-low power boost converter with battery management for energy harvester applications). An analogous chemical fuel cell system was realised by Palma and Enjeti [28] using modularised DC-DC converter connected to a modular PEM fuel cell stack.

The series connection of the stack was not conventional, as when connecting electrochemical batteries in series, but also involved cross bridging between the cells as explained in [22]. This did not affect the stack voltage, as it was able to deliver the cumulative voltage generated by each cells. What was more interesting in this study is that we are now able to utilise the stack voltage in order to power (in this case) a resistive load, while it delivered stable voltage (1.26 V) and current (2.52 mA), as long as the stack was sufficiently fed (Figure 5), which was the case until day 4. Figure 5 also reveals the daily cyclic temperature disturbances, evidenced by the control effort electrical loads applied by the control system. The presented study was carried out during the peak winter month of December, (UK) and the change in load (Figure 5c) coincides with the shorter daytime. MFCs that were connected to static loads showed this variation clearly (Figure S3 in *SI*). The controller was able to react to this

temperature variation by adjusting the controller load for individual MFCs and was able to sustain the voltage for each MFC1-4 for about 5 hours, after which the loadings resume roughly the previous levels preceding the sudden variation.

As it can be observed in Figure 5, the MFCs were operated at different level of loads (control effort) in order to achieve the same voltage level. This is due to the differences in the internal resistances of the MFCs, resulting from various physico-chemical factors. It is evident that the sequential order of the MFCs in the hydraulic regime did not coincide with the controlled load operational levels, though this might be the case in another arbitrary system. Furthermore, not all MFCs needed to be at the same voltage level in the stack (TEST 2 and TEST 3) in order to maintain proper stack operation without voltage reversals. It was previously thought that when MFCs are hydraulically linked in series, they should not be connected electrically in series, such as in the case of MFCs hydraulically concatenated in a single tube and sharing the same anolyte [20, 21]. Here, we have shown for the first time that it is possible to connect MFCs so that they are indeed hydraulically in series (sharing the same anolyte), and simultaneously connected electrically in series, without causing voltage reversal. Furthermore, the power has been drawn at the full stack voltage, which could be seen to be the cumulative sum of the individual MFCs within the stack. Further investigations to consider more abrupt and substantial variations temperature and organic loading are believed to be entirely appropriate to investigate the capacity of the control strategy to reject substantive fluctuation in operating conditions.

The control strategy presented herein is believed to be entirely transferable to a suitable microprocessor based technology, particularly one of several available integrated circuit (IC) microcontrollers with low power operating functionality. Alongside highly efficient MOSFET technology or specialist energy harvesting ICs,

that can utilise the regulatory power requiring dissipation or harvesting at each MFC controller. The digital controller can be placed in *sleep mode* for most of the time (*circa* 200µs 'awake' in a sampling interval (in this study) of 23 seconds, with a modest oscillator frequency of 16MHz) in comparison to a digitally implemented, continuous controller (0.5 seconds sampling interval in previous study [23]. This represents a 98% increase in *sleep mode* time with commensurate power saving. For example, an Atmel© 8-bit AVR Microcontroller, according to datasheets [29] can consume 0.2 mA with 1.8V supply and 1MHz clock, while Power-Down Mode (with watchdog timer disabled) can achieve 150nA. This and similar devices have the functionality and to implement the presented digital control strategy. Such power savings over large numbers of stacked BES devices may be significant. Therefore, the application of sampled-time digital control in the connectivity arrangement presented for controlling voltage, avoiding voltage reversal, reducing power consumption by the control system and harvesting power from MFCs, shows significant promise.

5. Conclusion

Control of MFC stacks has been considered by several researchers and accepted as a desirable pursuit, mainly due to the occurrence of the reversal of the cell voltage. In the presented study, cell voltage reversal was not observed; hence, it is possible to connect electrically in series, MFCs with hydraulically concatenated and electrically communicating anolyte chambers, such as tubular MFCs in this study without undergoing such cell voltage reversals. The results show that sampled-time digital control can be employed to maintain constant voltages in continuously fed MFC stacks of the same electrical and hydraulic connectivity, and despite differences in the MFC voltages within the stack, can generate a voltage equal to the aggregated cell voltages, and power consumption at this controlled potential is achievable. Hence, the

voltage of MFCs connected in series can be controlled individually and finally, the stack voltage produced can be utilised. The sampled-time controller performance was satisfactory as it was able to maintain consistent MFC voltages rejecting the variations caused by electrical loading, ambient temperature and the substrate depletion. The sampled time digital controller as presented is simple to implement and can be effectively embedded into widely available inexpensive microcontrollers and would reduce power consumption over an equivalent continuous control strategy.

ACKNOWLEDGEMENT

This work was supported by the Natural Environment Research Council (NERC) [grant number: NE/L014106/1]; through the Resource Recovery from Waste Programme, in the Microbial Electrochemical Technology for Resource Recovery (MeteoRR) project. This work was also part supported by the EPSRC Multi-disciplinary fuels, RCUK Energy programme [EP/N009746/1], Liquid fuels and bioenergy from CO_2 Reduction (Lifes-CO2R) project; and the FLEXIS research project (grant number: WEFO 80835).

References

[1] D. Pant, G. Van Bogaert, L. Diels, K. Vanbroekhoven, Bioresource Technology, 101 (2010) 1533-1543.
[2] J.C. Mankins, Acta Astronautica, 65 (2009) 1216-1223.
[3] Y. Dong, Y. Qu, W. He, Y. Du, J. Liu, X. Han, Y. Feng, Bioresource Technology, 195 (2015) 66-72.
[4] Z. Ge, Z. He, Environmental Science: Water Research & Technology, 2 (2016) 274-281.
[5] F. Zhang, Z. Ge, J. Grimaud, J. Hurst, Z. He, Environmental Science & Technology, 47 (2013) 4941-4948.
[6] L. Zhuang, Y. Yuan, Y. Wang, S. Zhou, Bioresource Technology, 123 (2012) 406-412.
[7] P. Aelterman, K. Rabaey, H.T. Pham, N. Boon, W. Verstraete, Environmental Science & Technology, 40 (2006) 3388-3394.
[8] J. An, B. Kim, I.S. Chang, H.-S. Lee, Journal of Power Sources, 278 (2015) 534-539.
[9] B. Kim, B.-G. Lee, B.H. Kim, I.S. Chang, ChemElectroChem, 2 (2015) 755-760.
[10] J. An, Y.S. Lee, T. Kim, I.S. Chang, Journal of Power Sources, 323 (2016) 23-28.
[11] N. Degrenne, B. Allard, F. Buret, F. Morel, S.E. Adami, D. Labrousse, in: Proceedings of the 2011 14th European Conference on Power Electronics and Applications, 2011, pp. 1-10.

[12] D. Sartori, D. Brunelli, in: 2016 IEEE Sensors Applications Symposium (SAS), 2016, pp. 1-6.
[13] P.K. Wu, J.C. Biffinger, L.A. Fitzgerald, B.R. Ringeisen, Process Biochemistry, 47 (2012) 1620-1626.
[14] J.D. Park, Z. Ren, IEEE Transactions on Energy Conversion, 27 (2012) 715-724.
[15] H. Wang, Z. Ren, J.-D. Park, Journal of Power Sources, 220 (2012) 89-94.
[16] I. Ieropoulos, J. Winfield, J. Greenman, Bioresource Technology, 101 (2010) 3520-3525.
[17] Y. Kim, M.C. Hatzell, A.J. Hutchinson, B.E. Logan, Energy & Environmental Science, 4 (2011) 4662-4667.
[18] M. Alaraj, M. Radenkovic, J.-D. Park, Journal of Power Sources, 342 (2017) 726-732.
[19] R. Umaz, C. Garrett, F. Qian, B. Li, L. Wang, IEEE Transactions on Power Electronics, PP (2016) 1-1.
[20] L. Zhuang, S. Zhou, Electrochemistry Communications, 11 (2009) 937-940.
[21] D. Kim, J. An, B. Kim, J.K. Jang, B.H. Kim, I.S. Chang, ChemSusChem, 5 (2012) 1086-1091.
[22] H.C. Boghani, G. Papaharalabos, I. Michie, K.R. Fradler, R.M. Dinsdale, A.J. Guwy, I. Ieropoulos, J. Greenman, G.C. Premier, Journal of Power Sources, 269 (2014) 363-369.
[23] H.C. Boghani, I. Michie, R.M. Dinsdale, A.J. Guwy, G.C. Premier, Journal of Power Sources, 322 (2016) 106-115.
[24] K. Mikhaylov, J. Tervonen, in: International Congress on Ultra Modern Telecommunications and Control Systems, 2010, pp. 1150-1156.
[25] I.A. Ieropoulos, A. Stinchcombe, I. Gajda, S. Forbes, I. Merino-Jimenez, G. Pasternak, D. Sanchez-Herranz, J. Greenman, Environmental Science: Water Research & Technology, 2 (2016) 336-343.
[26] J.R. Kim, G.C. Premier, F.R. Hawkes, R.M. Dinsdale, A.J. Guwy, Journal of Power Sources, 187 (2009) 393-399.
[27] J.A. Cruwys, R.M. Dinsdale, F.R. Hawkes, D.L. Hawkes, Journal of Chromatography A, 945 (2002) 195-209.
[28] L. Palma, P.N. Enjeti, IEEE Transactions on Power Electronics, 24 (2009) 1437-1443.
[29] Atmel, in: 8-bit AVR Microcontroller with 4/8K Bytes In-System Programmable Flash, Microchip Technology Incorporated, http://ww1.microchip.com/downloads/en/DeviceDoc/Atmel-8495-8-bit-AVR-Microcontrollers-ATtiny441-ATtiny841_Datasheet.pdf, (Accessed 20.03.17).

List of Figure Captions

Figure 1. (a) Digital voltage controller scheme. (b) Simplified schematic of the MFC stack. (c) Schematic of the MFC stack (tube 2-5 are identical to tube-1).

Figure 2. Model parameters (time constants, τ and steady-state gain, k_{ss}) from (a) MFC1, (b) MFC2, (c) MFC3, (d) MFC4 and (e) MFC5 step tests as per day 2, 5, 7 and 9. (f) Substrate concentration measured from MFC tube-1 effluent and the reservoir.

Figure 3. Plots showing (a) Set points (SP) and MFC voltages (b) Errors, Efforts and electrical loadings and, (c) controller gains and the controller sampling time during step tests.

Figure 4. Plots showing (a) Set points (SP) and MFC voltages and stack voltage; (b) Errors and; (c) controller loadings and the stack loading during the stack-loading test.

Figure 5. Plots showing (a) Set points (SP) and MFC voltages and stack voltage; (b) Errors and; (c) controller loadings and the stack loading during the long-term stack-loading test.